Ultrasonics Sonochemistry 18 (2011) 1118–1123

Contents lists available at ScienceDirect

Ultrasonics Sonochemistry

journal homepage: www.elsevier.com/locate/ultsonch

Room temperature synthesis of crystalline CeO_2 nanopowder: Advantage of sonochemical method over conventional method

Dipak Vitthal Pinjari, Aniruddha Bhalchandra Pandit *

Chemical Engineering Division, Institute of Chemical Technology, Matunga, Mumbai 400019, India

ARTICLE INFO

Article history:
Received 19 October 2010
Received in revised form 14 January 2011
Accepted 18 January 2011
Available online 28 January 2011

Keywords:
Ceria (CeO_2)
Nanomaterial
Sonochemical (acoustic cavitation) method

ABSTRACT

In the present study, nano-sized ceria (CeO_2) powders were prepared using conventional and sonochemically assisted precipitation method, without any stabilizers, using cerium nitrate as a starting material and sodium hydroxide as a precipitating agent. The synthesized ceria powders were characterized by XRD, TGA and SEM to determine crystallite size, % crystallinity, thermal weight loss and shape respectively. It was found that the crystallite size obtained in both the synthesis methods were below 30 nm. It was also found that sonochemical synthesis method is energy efficient method saving more than 92% of energy as compared to that utilized by the conventional synthesis method. There was also a significant reduction in the reaction duration.

1. Introduction

Ceria i.e. cerium dioxide (CeO_2), a crystalline materials, is a major compound in the useful rare earth family, and has received more attention in recent years due to many distinctive characteristics, such as unique ultraviolet radiation absorbing ability [1], high stability at higher temperature, high hardness index and its reactivity [2]. The ceria powders have been commercially developed to be used in various applications, like glass polishing material [3], catalytic support or promoter [4], oxygen ion conductor in solid oxide fuel cells (SOFCs) [5], gas sensor [6], UV absorbent [1] and abrasives of the CMP slurry in semiconductor fabrication [7]. Several researchers have published reports on the synthesis of ceria by using different methods such as sol–gel process [8,9], hydrothermal or solvothermal synthesis [10–14], forced hydrolysis [15], microemulsion [16], precipitation [17–20], etc. Different precursors [21–23] have also been used for the synthesis of ceria powder such as $Ce_2O(CO_3)_2{\cdot}H_2O$, $Ce(NO_3)_3{\cdot}9H_2O_3$, and $Ce(NO_3)_3{\cdot}6H_2O$. Yin et al. [24] have reported sonochemical synthesis of ceria powder using different stabilizers, solvents and cosolvents.

The sonochemical method has been proved to be a useful method to obtain novel materials [25,26]. The chemical effects of ultrasonic irradiation arise from acoustic cavitation, in other words, the formation, growth and implosive collapse of bubbles in a liquid medium, which results in an instantaneously high temperature and pressure pulse [27,28]. These special conditions of high temperature, pressure and local intense micromixing attained during acoustic cavitation lead to many unique properties in the irradiated solution and particles suspended in the same [29].

In this paper, ceria nanopowder was synthesized using conventional (NUS) and sonochemical (US) assisted precipitation technique. The effect of ultrasound on % crystallinity, crystallite size, % weight loss and morphology of the synthesized CeO_2 has been studied to understand the advantage of ultrasound (input ultrasonic energy) in the synthesis of CeO_2.

2. Materials and methods

2.1. Materials

Cerium nitrate hexahydrate (AR) precursor was obtained from S. d. Fine Chemicals Ltd., Mumbai, India. Sodium hydroxide (AR) was obtained from Merck Ltd., Mumbai, India.

2.2. Ultrasound set-up

Ultrasound for sonochemical synthesis is generated with the help of ultrasonic instrument set up (horn type). The schematic of the set up is given in Fig. 1. The specification and details of the set up, processing parameters used during the experiments are:

Make: Ace, USA.

Operating frequency: 22 kHz, rated output power: 750 W, diameter of stainless steel tip of horn: 1.3×10^{-2} m, surface area of ultrasound irradiating face: 1.32×10^{-4} m^2, expected ultrasound intensity: 3.4×10^5 W/m^2.

* Corresponding author. Tel.: +91 22 3361 2012; fax: +91 22 4145614.
E-mail address: dr.pandit@gmail.com (A.B. Pandit).

1350-4177/$ - see front matter © 2011 Elsevier B.V. All rights reserved.
doi:10.1016/j.ultsonch.2011.01.008

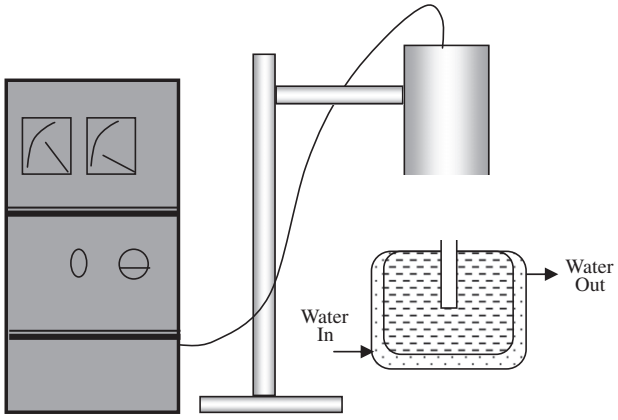

Fig. 1. Ultrasonic equipment.

2.3. Synthesis of CeO_2 by conventional method (NUS)

Cerium nitrate hexahydrate, 0.9 g (0.1 gmol) was dissolved in 30 ml distilled water and 0.24 g, (0.3 gmol) sodium hydroxide was dissolved in 30 ml distilled water separately and was kept ready. The sodium hydroxide solution was then added drop wise to the cerium nitrate hexahydrate solution under constant stirring using a magnetic stirrer (Model RQ1210, Remi Metals Gujarat Limited, India). The aqueous clear solutions turned yellowish white initially but as the reaction proceeds, it converts into light yellow colloidal suspension. The reaction was allowed to proceed for 4 h after the complete addition of sodium hydroxide solution under stirring at room temperature (35 ± 2 °C). The temperature of the reaction mixture was maintained at 35 ± 2 °C by circulating water in jacketed reactor which was used for the synthesis work. The addition time of sodium hydroxide solution was about 2 min. After 4 h, the solution was centrifuged at 12000 rpm for 10 min to separate the product and the settled product was washed thrice using distilled water to remove the byproducts. After complete washing, the product was dried at 100 °C for 3 h to complete the conversion of $Ce(OH)_3$ to CeO_2. After complete conversion, CeO_2 powder obtained was (light yellowish in nature), cooled, ground by mortar, checked for yield and characterized by XRD, TGA and SEM analysis. The synthesis of CeO_2 material by conventional method (NUS) was replicated thrice and the results were computed by averaging the individual results and were displayed with error bar (± variation) for % yield, % crystallinity and crystallite size.

2.4. Synthesis of CeO_2 by sonochemical method (US)

Cerium nitrate hexahydrate, 0.9 g (0.1 gmol) was dissolved in 30 ml distilled water and 0.24 g, (0.3 gmol) sodium hydroxide was dissolved in 30 ml distilled water separately and was kept ready. The **s**odium hydroxide solution was then added drop wise to the cerium nitrate hexahydrate solution under sonication using an Ultrasonic Horn (ACE 22 kHz) at 40% amplitude for 2 min with a 5 s pulse and 5 s relaxation cycle at time $t = 0$ h. Care was taken to see to it that the addition was done in conjunction with the sonic pulse afforded by the transducer (Horn). After addition, the solution was again exposed to acoustic cavitation (by using ultrasonic horn) for further 18 min, by keeping all sonication parameters constant **(**same as that was used during mixing**)**, to carry out the complete reaction of cerium nitrate hexahydrate with sodium hydroxide. The temperature of the reaction mixture was maintained at 35 ± 2 °C by circulating water in jacketed reactor which was used for synthesis work. The rest of the procedure was the same as described before in Section 2.3.

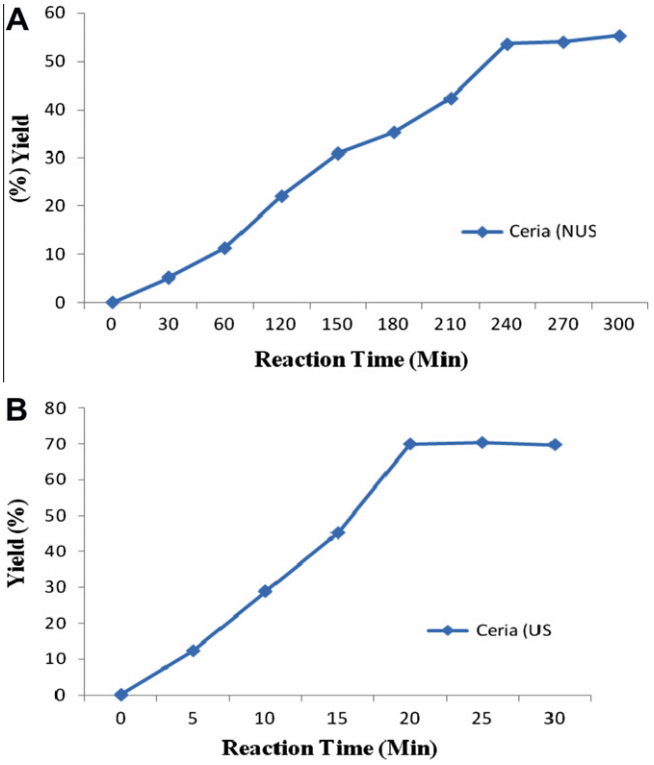

Fig. 2. Yield (%) of synthesized CeO_2 by (A) NUS method and (B) US method.

3. Characterizations

The dried CeO_2 samples (powder form) were first characterized by studying their X-ray Diffraction patterns on a Rigaku Mini-Flex X-ray Diffractometer. XRD patterns were recorded at angles between 2° and 80°, with a scan rate of 2°/min. Particle sizes were determined using the Debye–Scherrer equation. Thermogravimetric analysis (TGA) studies were performed using Thermal Analyser (TA Instruments, USA). The sample was heated in N_2 atmosphere in alumina crucible at the rate of 20 K/min. Sample preparation for Scanning Electron Microscopy (SEM) includes the deposition of platinum on CeO_2 powder. Scanning Electron Microscopy of the samples was carried out on a JOEL JSM 680LA 15 kV SEM to estimate the surface characteristics of the sample. Together, the XRD and SEM methods are expected to provide exact knowledge regarding the particle size and crystalline characteristics of the synthesized CeO_2.

4. Results

4.1. Yield and reaction time

It is already mentioned in Sections 2.3 and 2.4 that the reaction time taken for the conventionally synthesized CeO_2 was 4 h while reaction time taken for sonochemically synthesized CeO_2 was 20 min. It was found that 4 h time is optimum for NUS synthesized CeO_2 chalcone as the further enhancement in the % yield was not observed while in case of US synthesized CeO_2 20 min was optimum reaction time to get the highest yield (Fig. 2). The percentage yield of the reaction was estimated on the basis of initial weight of the raw materials taken and final weight of product obtained after the complete drying (compared to the stoichiometrically expected quantity). During the washing of synthesized CeO_2 material, unreacted raw materials present in the reaction and byproduct formed was separated. It was observed that yield of the reaction in the case

of sonochemically (US) synthesized CeO_2 (70.12 ± 1%) was higher than in the case of conventionally (NUS) synthesized CeO_2 (53.67 ± 1.74%). The error (± variation) is less than 2% for conventionally (NUS) synthesized CeO_2 and 1% for sonochemically (US) synthesized CeO_2. The impact of acoustic cavitation was evident in not only in the increased yields (yield is increased by 30% with a saving of 220 min reaction time) but also the reduction in average particle size (Table 1). This is due to the rapid micromixing and resulting faster reaction (also possibly due to the formation of hot spots) to form nano CeO_2. The reason for this is probably the fast kinetics of the US reaction providing not enough time for particle nucleation and growth and thus a reduced average particle size.

4.2. Crystallinity and crystallite size of CeO_2

X-ray diffraction is a versatile, non-destructive analytical method for identification and quantitative determination of various crystalline forms, known as 'phases' of compound present in powder and solid samples. Diffraction occurs as waves interact with a regular precipitated solid matrix structure whose repeat distance is about the same as the wavelength.

For the NUS and US synthesized CeO_2 samples, the XRD pattern (Fig. 3) shows four main reflections (111), (200), (220) and (311) characteristic of CeO_2 cubic phase with fluorite structure (Ref. JCPDS card 34-394). NUS sample may be having faced centered cubic structure and such samples shows maximum peaks.

From the XRD patterns (Fig. 3), it is also possible to compute the % crystallinity and crystallite size. The amorphous phase fraction of the sample may be determined by taking the ratio of the amorphous area (area not under the peaks) of the X-ray diffractogram to the total area. The area covered by the amorphous region means that the area of the diffractogram not contained by any sharp diffraction peaks. A method for estimation of amorphous phase fraction from XRD patterns have been developed by Prasad et al. [25,26] in our earlier work.

Crystallite size of the metal oxide samples may be obtained using the Debye–Scherrer equation. Vigneshwaran et al. [30,31] have used the Debye–Scherrer equation successfully for the estimation of size of nano ZnO in the past. The same procedure has been followed here. The Debye–Scherrer equation is used frequently in X-ray analysis of materials, particularly powder diffraction of metal oxides. It relates the peak breadth of a specific phase of a material to the mean crystallite size of that material. It is quantitative equivalent of saying that the larger the material's crystallites are, sharper are the XRD peaks. According to the full width at half-maximum (FWHM) of the diffraction peaks, the average size of the particles (crystallite) are estimated from the Scherrer equation.

All the computed results including % crystallinity and crystallite size have been tabulated in Table 1. XRD pattern of synthesized CeO_2 for both NUS and US process exactly matches with the XRD pattern of CeO_2. Also the peaks at different crystal planes of US synthesized CeO_2 matches exactly with that of NUS synthesized CeO_2 indicating essentially no difference with respect to the type of crystalline phase in the two products. The crystallinity of all the samples is still substantial because of the inherent characteristics of the sonically assisted process. It was found that NUS

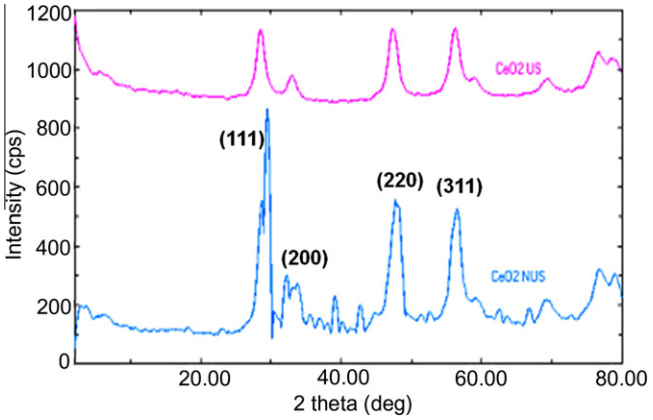

Fig. 3. XRD pattern of the conventionally (NUS) and sonochemically (US) synthesized CeO_2.

synthesized CeO_2 shows more crystallinity than US synthesized CeO_2. This may be because of adverse environments created during sonication and facilitating faster reaction, not allowing the nucleation and crystal growth to occur fully. The local high energy dissipation rate due to cavitation phenomenon and micromixing caused by the incorporation of acoustic cavitation as a reaction aid, may increase the randomness of the Brownian motion of the CeO_2 molecules not allowing regular crystal formation. This reduces the ability of the molecules to remain in a stable lattice positions for long, leading to the lowering of crystallinity. The peak broadening in the XRD pattern (for both samples) clearly indicates that very small nanocrystals are present in the samples. The peaks intensity in case of NUS synthesized CeO_2 is more than the peaks intensity of US synthesized CeO_2 which clearly indicates the presence of larger crystals for NUS synthesized CeO_2. Crystallite size of the US synthesized CeO_2 was found also to be significantly (6 nm against 30 nm) lower than NUS synthesized CeO_2. It could also be due to the reduction in crystallinity. As the crystallinity of metal oxide reduces, its crystallite size is also known to reduce, which is consistent with the observations reported in our earlier work. [25]

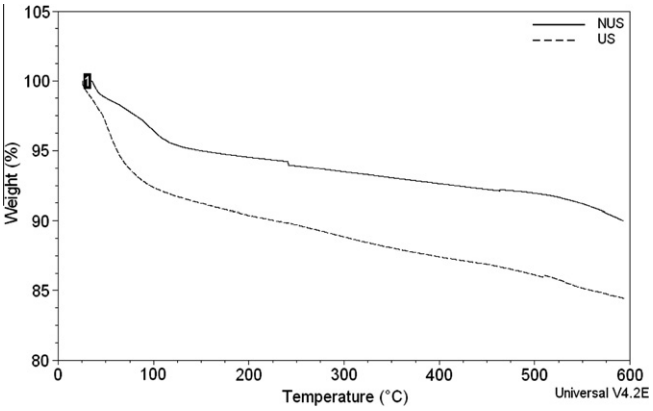

Fig. 4. TGA graph of the conventionally (NUS) and sonochemically (US) synthesized CeO_2.

Table 1
%Crystallinity, crystallite size and %yield of the conventionally (NUS) and sonochemically (US) synthesized CeO_2.

Method	Crystallinity (%)		Crystallite size *d* (nm)		Yield (%)		Energy (J)	Power input (W)
	Average	± variation	Average	± variation	Average	± variation		
Conventional	36.03	1.52	27	2	53.67	1.74	–	–
Sonochemical	21.44	2.15	6	1	70.12	1	37047	30.87

Table 2
%Weight loss of the conventionally (NUS) and sonochemically (US) synthesized CeO_2 with respect to temperature.

Temperature, °C	Weight remained (%)	
	NUS	US
R.T. (35)	100	100
50	98.78	96.89
100	96.39	92.31
150	94.99	91.19
200	94.51	90.34
250	93.89	89.68
300	93.47	88.83
350	93.05	88.03
400	92.67	87.39
450	92.20	86.86
500	91.93	86.10
550	91.19	85.17

4.3. Thermogravimetric analysis (TGA)

The thermogravimetric (TGA) analysis (Fig. 4) shows the weight loss of synthesized CeO_2 sample. It has been observed (Table 2) that continuous weight loss was occurred for both the samples (NUS and US synthesized CeO_2). At 50 °C, it has been observed that weight for NUS and US synthesized CeO_2 are 1.22% and 3.11%, respectively. As the both samples get heated at 139 °C, again notable weight loss was found. It is 3.61% for NUS synthesized CeO_2 and 7.69% for US synthesized CeO_2, when the water molecules (H_2O) start to disassociate themselves from $Ce(OH)_3$. It has been found that at 550 °C, total weight loss for NUS and US synthesized CeO_2 was 8.81% and 14.83% respectively. Uses of ultrasound to the reaction mixture are changing their crystallography. And as explained in Section 4.2, the high energy generated due to cavitation phenomenon and micromixing caused by the same may increase the randomness of the Brownian motion of the CeO_2 molecules not allowing regular crystal formation which leads to a decrease in thermal stability of the CeO_2 which is confirmed by weight loss observed for US process. Here, by observing results obtained in terms of % crystallinity, crystallite size and % weight loss for both the samples (NUS and US synthesized CeO_2), we feel that as the crystallinity of the metal oxide decreases, its size is also found to be lowered and increased weight loss. Another possible reason behind the higher weight loss observed in case of US synthesized CeO_2 may be attributed to the formation of agglomeration due to high energy. Enomoto et al. [32] and Prasad et al. [26] have reported that due to ultrasound irradiation, system consisting of suspended particles can cause agglomerations. This may be attributed to the formation of Ce–O–Ce bonds by combination reaction of Ce–OH bonds present on the surface of the particle species. This reaction is referred to as water condensation reaction [32,33].

$$Ce{-}OH + OH{-}Ce \rightarrow Ce{-}O{-}Ce + H_2O \quad (1)$$

These bonds are created by ultrasound enhanced high intensity collisions occurring between these particles in solution. The above mentioned observation of higher weight loss in the case of US synthesized sample could be due to this phenomenon.

Another possible reason behind the weight loss observed in US synthesized CeO_2 may be that as the average particle sizes

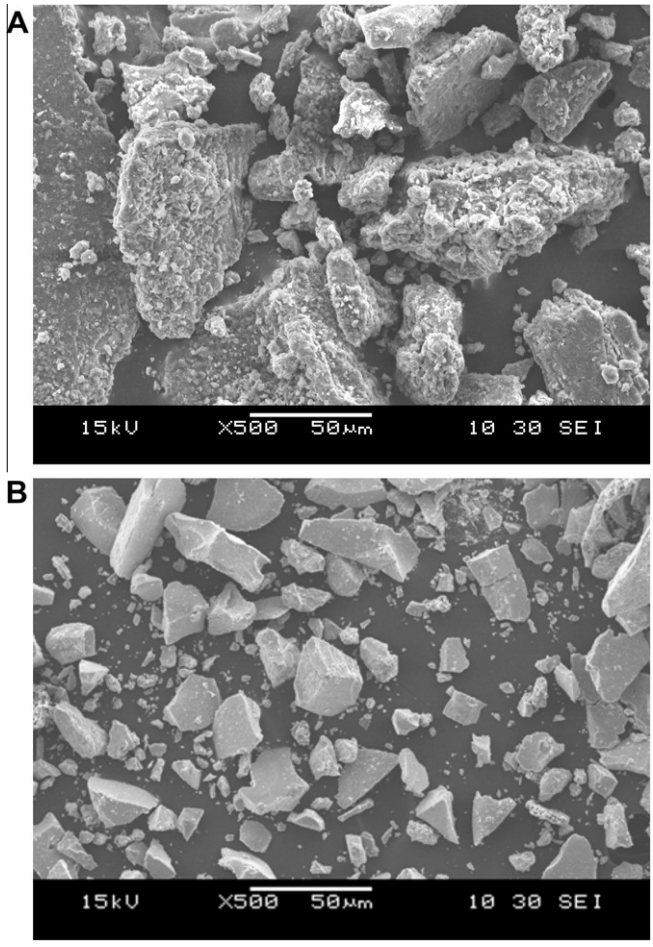

Fig. 5. SEM micrograph of synthesized CeO_2 at 500×: (A) conventionally (NUS) (B) sonochemically (US).

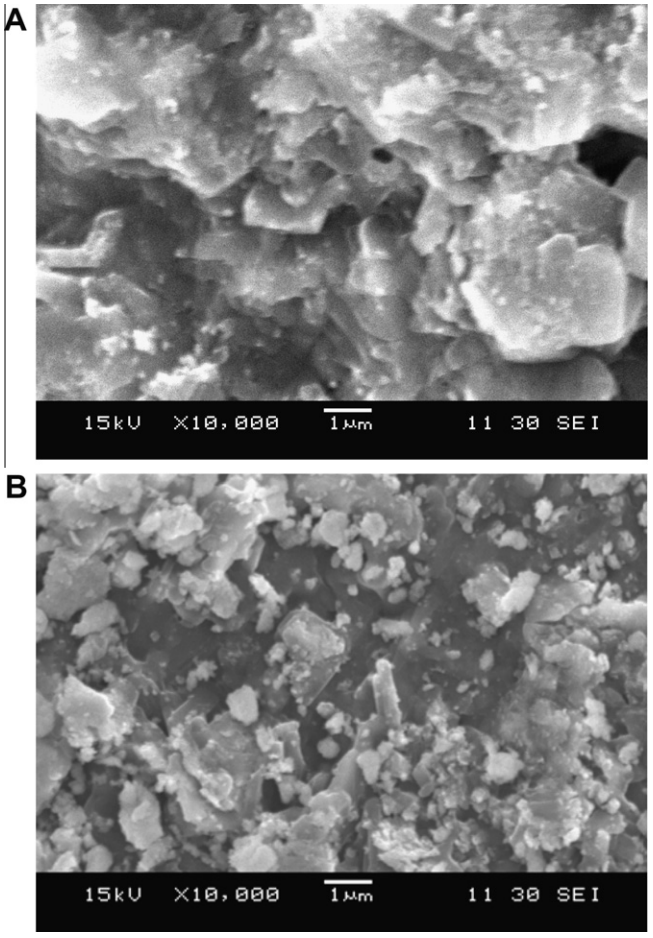

Fig. 6. SEM micrograph of synthesized CeO_2 at 10,000×: (A) conventionally (NUS) (B) ultrasonically (US).

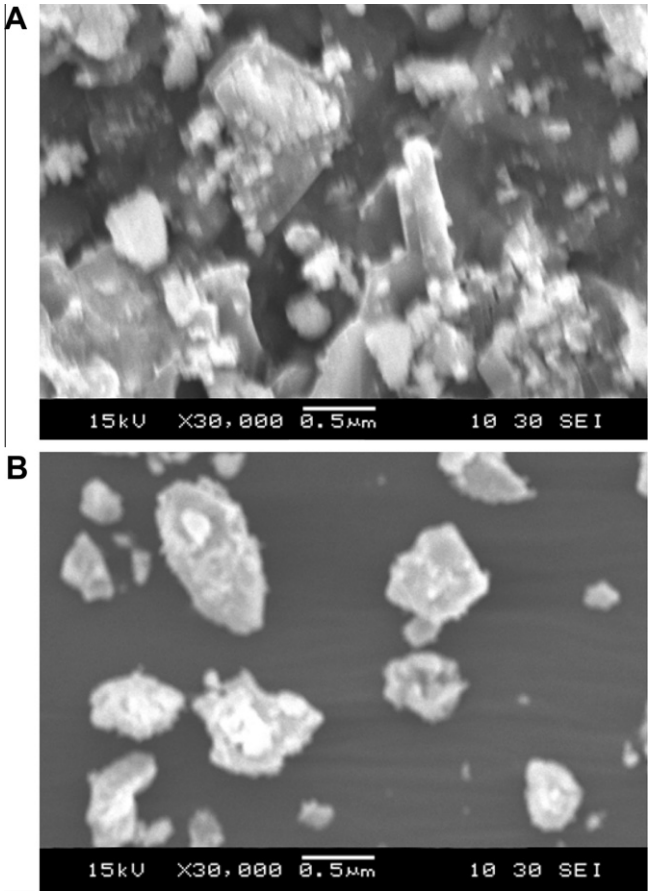

Fig. 7. SEM micrograph of synthesized CeO_2 at 30,000×: (A) conventionally (NUS) (B) ultrasonically (US).

observed for the CeO_2 synthesized by the US process is lower, it will conduct thermal radiation more efficiently and thus at a lower temperature it would feel a more significant effect of thermal convective currents leading to a possible phase transformation and thus weight loss can happen. However, more work needs to be carried out before it can be conclusively said so.

4.4. Scanning electron microscopy (SEM)

From the SEM micrographs (Figs. 5–7) of the NUS and US synthesized CeO_2 samples some observations have been made, that supported the results observed from the XRD patterns. We have compared the SEM image results of the CeO_2 for NUS (Fig. 5A) and US (Fig. 5B) at the same magnification of 500X. The US synthesized CeO_2 shows not only comparatively smaller particle size but also considerably less agglomeration. Here, we have interestingly observed that structure of NUS synthesized CeO_2 consists of small particles aggregated with larger particles but this is not observed for US synthesized CeO_2 material. These particles are smooth and sharp cuts (US synthesized) as compared to NUS synthesized particles. This may be due to active surface charge present on NUS synthesized CeO_2 material, resulting in agglomerated particles which may be lost in case of US synthesized CeO_2 material because of local higher energy dissipation and shock waves, generated by ultrasound at a higher magnification of 10,000X. Lesser agglomeration and uneven shaped structures are observed in the case of the US samples in general rather than the agglomerated looking particles for NUS sample.

Use of cavitation as a reaction aid has had its influence in the reaction step by considerably reducing their particle size and increasing the packing of these particles into other composite systems. This not only helps in improving its effect on material properties by increasing the effective surface area, reducing the overall reaction time but also aids in increasing the different types of crystals formed.

5. Energy efficacy

For the comparison of the energy required for these two synthesis methods (conventional (NUS) and sonochemical (US)) to obtain CeO_2 nanomaterials, a sample calculation is reported in Appendix (I). We have already reported the work done on the energy efficacy of the conventional and sonochemical processes. [25,34] The energy utilized for the synthesis of CeO_2 nanomaterial is the total energy supplied (kJ) per unit weight of the material processed/obtained (g). It is already explained in Section 4.1 that reaction time to synthesize ZnO were 20 min for US method and 4 h NUS method. Total energy required per unit weight of the material obtained to synthesize CeO_2 is 15.15×10^{-2} (kJ/g) for US synthesis method and 200.43×10^{-2} (kJ/g) for NUS synthesis method.

Thus, US synthesis method has proved to be an energy efficient method which saved more than 92% of energy utilized by NUS synthesis method along with the reduced in the reaction duration.

6. Conclusions

Nanostructured CeO_2 particles were successfully synthesized, at room temperature, without stabilizers, by conventional (NUS) and sonochemical method (US). The sonochemical synthesis method has saved substantial energy (more than 92%) for the synthesis of CeO_2. Thus, the sonochemical synthesis technique is fast, simple, convenient, time saving, economical, and environmentally benign. We believe that this method promises us a future large-scale synthesis for many applications in nanotechnology field.

Appendix A. Energy calculations

A.1. Energy delivered during sonication

- Energy delivered during sonication = energy required to synthesize CeO_2 material.
- Electrical energy delivered during sonication using horn for 20 min (indicated by the power meter) = 37.047 kJ.
- Efficiency of horn taken for the calculation = 30% (estimated independently using calorimetric studies).
- Actual energy delivered by horn during sonication = energy delivered during sonication using horn in 10 min × Efficiency of horn = 37.047 × 30/100 = 9.2617 kJ = 9.26 kJ.
- Quantity of material processed = quantity of water + quantity of cerium nitrate hexahydrate + quantity of sodium hydroxide = 60 g (60 ml) + 0.9 g + 0.24 g = 61.14 g.
- Net energy supplied for processing of material using sonochemical method = actual energy delivered by horn during sonication/quantity of material processed = 9.26 (kJ)/61.14 (g) = 15.15×10^{-2} (kJ/g) (A)

A.2. Energy delivered during conventional method

- Voltage input in magnetic stirrer (Model RQ1210, Remi Metals Gujarat Limited, India) = 230 V.
- Current measured using digital multimeter (KUSAM-MECO Model 2718, Kusam Electrical Industries Ltd., Mumbai, India) = 37 mA = 37×10^{-3} A.
- Power input in overhead stirrer = voltage input × current measured = 230 (V) × 37×10^{-3} (A) = 8.51 W (J/s).

- Time required for completion of reaction = 4 h (14,400 s).
- Net energy delivered during conventional method = power input in magnetic stirrer × time required for completion of reaction = 8.51 J/s × 4 h × 3600 s/h = 122,544 J = 112.544 kJ.
- Quantity of material processed = quantity of water + quantity of zinc nitrate hexahydrate + quantity of sodium hydroxide = 60 g (60 ml) + 0.9 g + 0.24 g = 61.14 g.
- Net energy supplied for processing of material using conventional method = net energy delivered during conventional method/quantity of material processed = 112.544 (kJ)/61.14 (g) = 200.43×10^{-2} (kJ/g) (B).

A.3. Energy saved

- Net energy saved = (net energy supplied for processing of material using conventional method (B)) − (net energy supplied for processing of material using sonochemical method (A)) = 200.43×10^{-2} (kJ/g) − 15.15×10^{-2} (kJ/g) = 185.28×10^{-2} (kJ/g).

References

[1] S. Tsunekawa, R. Sahara, Y. Kawazoe, A. Kasuya, Origin of the blue shift in ultraviolet absorption spectra of nanocrystalline CeO_{2-x} particles, Mater. Trans. JIM 41 (2000) 1104–1107.

[2] A. Trovarelli, C. de Leitenburg, M. Boaro, G. Dolcetti, The utilization of ceria in industrial catalysis, Catal. Today 50 (1999) 353–367.

[3] S.H. Lee, Z.Y. Lu, S.V. Babu, E. Matijevic, Chemical mechanical polishing of thermal oxide films using silica particles coated with ceria, J. Mater. Res. 17 (2002) 2744–2749.

[4] E. Bekyarova, P. Fornasiero, J. Kaspar, M. Graziani, CO oxidation on Pd/CeO_2–ZrO_2 catalysts, Catal. Today 45 (1998) 179–186.

[5] H. Yahiro, Y. Baba, K. Eguchi, H. Arai, High temperature fuel cell with Ceria–Yttria solid electrolyte, J. Electrochem. Soc. 135 (1988) 2077–2080.

[6] N. Izu, W. Shin, N. Murayama, S. Kanzaki, Resistive oxygen gas sensors based on CeO_2 fine powder prepared using mist pyrolysis, Sens. Actuator B: Chem. 87 (2002) 95–98.

[7] M. Jiang, N.D. Wood, R. Komanduri, On the chemo-mechanical polishing (CMP) of Si_3N_4 bearing balls with water based CeO_2 slurry, J. Eng. Mater. Technol.: Trans. ASME 120 (1998) 304–312.

[8] X. Chu, W. Chung, L.D. Schmidt, Sintering of sol–gel-prepared submicrometer particles studied by transmission electron microscopy, J. Am. Ceram. Soc. 76 (1993) 2115–2118.

[9] A. Makishima, H. Kubo, K. Wada, Y. Kitami, T. Shimohira, Yellow coatings produced on glasses and aluminum by the sol–gel process, J. Am. Ceram. Soc. 69 (1986) C127–129.

[10] Y. Hakuta, S. Onai, H. Terayama, T. Adschiri, K. Arai, Production of ultra-fine ceria particles by hydrothermal synthesis under supercritical conditions, J. Mater. Sci. Lett. 17 (1998) 1211.

[11] N.C. Wu, E.W. Shi, Y.Q. Zheng, W.J. Li, Effect of pH of medium on hydrothermal synthesis of nanocrystalline cerium(IV) oxide powders, J. Am. Ceram. Soc. 85 (2002) 2462–2468.

[12] M. Hirano, E. Kato, Hydrothermal synthesis of nanocrystalline cerium(IV) oxide powders, J. Am. Ceram. Soc. 82 (1999) 786–788.

[13] N. Uekawa, M. Ueta, Y.J. Wu, K. Kakegawa, Synthesis of CeO_2 spherical fine particles by homogeneous precipitation method with polyethylene glycol, Chem. Lett. 31 (2002) 854–855.

[14] E. Verdon, M. Devalette, G. Demazeau, Solvothermal synthesis of cerium dioxide microcrystallites: effect of the solvent, Mater. Lett. 25 (1995) 127–131.

[15] X.T. Dong, G.Y. Hong, D.C. Yu, D.S. Yu, Synthesis and properties of cerium oxide nanometer powders by pyrolysis of amorphous citrate, J. Mater. Sci. Technol. 13 (1997) 113–116.

[16] T. Masui, K. Fujiwara, K. Machida, G. Adachi, T. Sakata, H. Mori, Characterization of cerium(IV) oxide ultrafine particles prepared using reversed micelles, Chem. Mater. 9 (1997) 2197–2204.

[17] X.D. Zhou, W. Huebner, H.U. Anderson, Room-temperature homogeneous nucleation synthesis and thermal stability of nanometer single crystal CeO_2, Appl. Phys. Lett. 80 (2002) 3814–3816.

[18] B. Aiken, W.P. Hsu, E. Matijevic, Preparation and properties of monodispersed colloidal particles of lanthanide compounds: III, Yttrium(III) and mixed Yttrium(III)/cerium(III) systems, J. Am. Ceram. Soc. 71 (1988) 845–853.

[19] P.L. Chen, I.W. Chen, Reactive cerium(IV) oxide powders by the homogeneous precipitation method, J. Am. Ceram. Soc. 76 (1993) 1577–1583.

[20] B. Djuricic, S. Pickering, Nanostructured cerium oxide: preparation and properties of weakly-agglomerated powders, J. Eur. Ceram. Soc. 19 (1999) 1925–1934.

[21] Joon-Sung Lee, Jin-Seok Lee, Sung-Churl Choi, Synthesis of nano-sized ceria powders by two-emulsion method using sodium hydroxide, Mater. Lett. 59 (2005) 395–398.

[22] Huey-Ing Chen, Hung-Yi Chang, Homogeneous precipitation of cerium dioxide nanoparticles in alcohol/water mixed solvents, Colloids Surf. A: Physicochem. Eng. Aspects 242 (2004) 61–69.

[23] Emanuel Kockrick, Christian Schrage, Anett Grigas, Dorin Geiger, Stefan Kaskel, Synthesis and catalytic properties of microemulsion-derived cerium oxide nanoparticles, J. Solid State Chem. 181 (2008) 1614–1620.

[24] Lunxiang Yin, Yanqin Wang, Guangsheng Pang, Yuri Koltypin, Aharon Gedanken, Sonochemical synthesis of cerium oxide nanoparticles – effect of additives and quantum size effect, J. Colloid Int. Sci. 246 (2002) 78–84.

[25] K. Prasad, D.V. Pinjari, A.B. Pandit, S.T. Mhaske, Phase transformation of nanostructured titanium dioxide from anatase-to-rutile via combined ultrasound assisted sol–gel technique, Ultra Sonochem. 17 (2010) 409–415.

[26] K. Prasad, D.V. Pinjari, A.B. Pandit, S.T. Mhaske, Synthesis of titanium dioxide by ultrasound assisted sol–gel technique: effect of amplitude (power density) variation, Ultra Sonochem. 17 (2010) 697–703.

[27] V.S. Moholkar, S.P. Sable, A.B. Pandit, Mapping the cavitation intensity in an ultrasonic bath using the acoustic emission, AIChE J. 46 (2000) 684–694.

[28] A.V. Mahulkar, C. Riedel, P.R. Gogate, U. Neis, A.B. Pandit, Effect of dissolved gas on efficacy of sonochemical reactors for microbial cell disruption: experimental and numerical analysis, Ultra Sonochem. 16 (2009) 635–643.

[29] D.V. Pinjari, A.B. Pandit, Cavitation milling of natural cellulose to nanofibrils, Ultra Sonochem. 17 (2010) 845–852.

[30] N. Vigneshwaran, K. Sampath, A.A. Kathe, P.V. Varadarajan, V. Prasad, Functional finishing of cotton fabrics using zinc oxide-soluble starch nanocomposites, Nanotechnology 17 (2006) 5087–5095.

[31] S. Chandramouleeswaran, S.T. Mhaske, A.A. Kathe, P.V. Varadarajan, V. Prasad, N. Vigneshwaran, Functional behaviour of polypropylene/ZnO-soluble starch nanocomposites, Nanotechnology 18 (2007) (art. no. 385702).

[32] N. Enomoto, T. Koyano, Z. Nakagawa, Effect of ultrasound on synthesis of spherical silica, Ultra Sonochem. 3 (1996) S105–S109.

[33] R.L. Frost, M. Daniel Lisa, Z. Huaiyong, Synthesis and characterization of clay-supported titania photocatalysts, J. Colloid Int. Sci. 316 (2007) 72–79.

[34] K.J. Jarag, D.V. Pinjari, A.B. Pandit, G.S. Shankarling, Synthesis of chalcone (3-(4-fluorophenyl)-1-(4-methoxyphenyl)prop-2-en-1-one): advantage of sonochemical method over conventional method, Ultra Sonochem. 18 (2011) 617–623.